

How to make a fluoropolymer sticky!

Hadi Izadi and Alexander Penlidis

Department of Chemical Engineering, Institute for Polymer Research, University of Waterloo,
Waterloo, ON, Canada N2L 3G1

The non-reactivity along with low surface energy lead to very weak adhesion and friction of fluoropolymers, making them ideal candidates for fabrication of non-sticky and releasing surfaces. However, possessing low dielectric constants and high electronegativity fluorine-based units, fluoropolymers can become highly charged at the surface upon contact with other materials via the so-called contact electrification phenomenon, leading to formation of electrostatic interactions at the surface. The electrostatic forces developed via contact electrification (the same incident that generate charges over a piece of amber when it is rubbed against wool) can generate large work of adhesion which is even comparable to the fracture energies of ionic-covalent materials.¹⁻³ In view of that and considering that an efficient triboelectric charging requires enhanced actual area of contact, for the first time, we have fabricated a novel electrostatic-based dry adhesive by developing high aspect-ratio (AR) nanopillars on a rigid fluoropolymer (Teflon AF).⁴⁻⁶ Due to the extremely high AR of nanopillars which are terminated at the tip with a peculiar (fluffy) sheet-like nanostructure (inspired by the sticky fibrillar structure of gecko lizard foot pads) (see Figure 1), the fabricated dry adhesive can come into an ultimate contact, leading to enhanced adhesion and friction. Unlike gecko and other synthetic dry adhesives, which require efficient van der Waals interactions upon contact, the fabricated dry adhesive is the only one of its kind which relies for the most part on electrostatic interactions.⁴⁻⁶

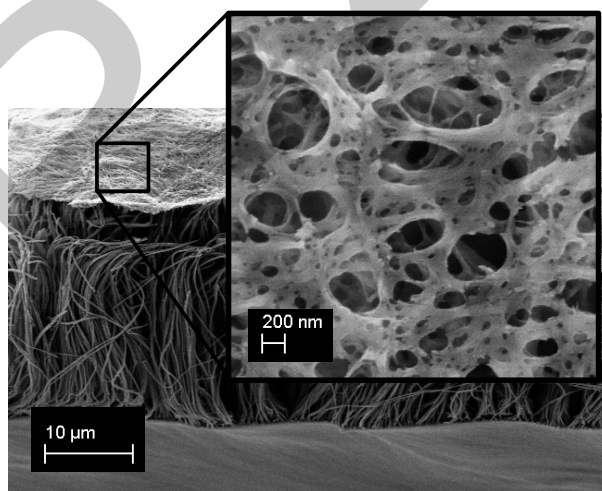


Figure 1. SEM image of bi-level Teflon AF nanopillars (45°-view). Extremely high AR Teflon AF nanopillars (200 nm in diameter) are terminated at the tip with a unique fluffiness nanostructure. The magnified image is from the top-view.⁶

In this research, bi-level nanopillars of various heights and hierarchy features (as a dry adhesive) were fabricated from Teflon AF 1600 (DuPont) by using anodic aluminum oxide (AAO) membranes (0.2 μm pore diameter, 60 μm thick, pore density 25-50 %; Whatman Inc.) as the mold. As shown in Figure 2, the polymer granules were placed over the AAO membrane and,

subsequently, the polymer and the mold were heated from the bottom to reach the constant desired "heating temperature" above the glass transition temperature of the polymer ($T_g = 160$ °C).⁷ From the top, the polymer was cooled down by setting the "cooling temperature" at a temperature much lower than the glass transition temperature of the polymer.

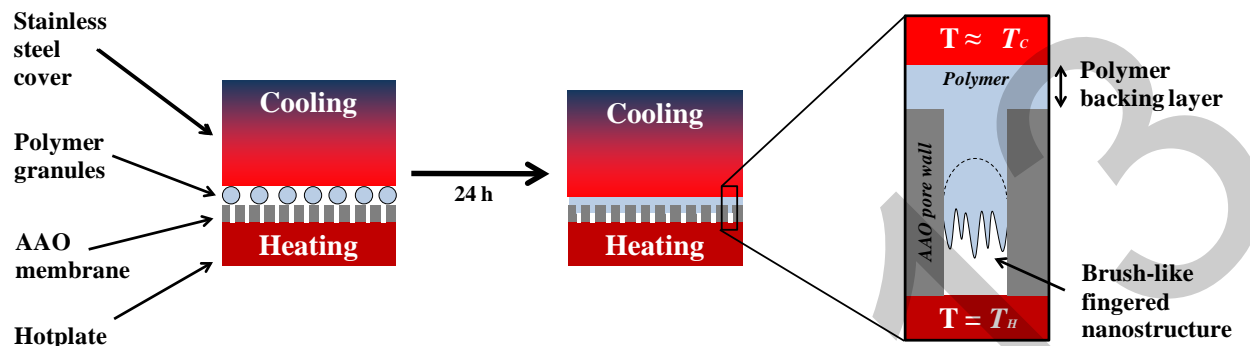


Figure 2. Schematic of the procedure for fabrication of bi-level Teflon AF nanopillars. The precursor film of the polymer melt, which was formed at the forehead of the developing polymer melt confined within AAO nanopores, fingered over the pore walls. Upon removal of the mold, the collapse and entanglement of the developed brush-like nanostructure led to formation of a fluffy nanostructure on top of the base Teflon AF nanopillars.

Upon infiltration of the Teflon AF melt into the AAO nanopores at elevated temperatures, like other polymers, the polymer melt spread over the pore walls (because of the large difference in surface energy of the polymer and the mold) and formed a thin nanoscopic precursor film at the forehead of the developing polymer melt. However, due to the very low surface energy of the polymer (15.7 mJ/m^2),⁷ the thermocapillarity-driven stresses at the contact line of the precursor film have led to instability of the precursor film and its fingering over the pore walls (Figure 2).⁴⁻⁶ The very soft nanostructure of the developed brush-like hierarchical level, after solidification of the polymer and dissolving the mold in NaOH solution (1.25 M), instantly collapsed during the drying step, resulting in formation of an exceptional fluffy nanostructure on top of the base nanopillars of $\sim 200 \text{ nm}$ in diameter (see Figure 1). As drying continued, the sheet-like nanostructure, with sufficiently high density and large size, held the tip of the base nanopillars away from each other and, accordingly, hindered the lateral collapse at the tips during the drying step (see Figure 1).⁴⁻⁶

In the current fabrication method, by enhancing the "heating temperature" and keeping the "cooling temperature" constant (i.e., increasing the temperature gradient), the size (length and width) of the hierarchical fingered brushes was decreased while their density increased. In addition to size and density of the fingered brushes, adjusting the heating temperature also altered the infiltration depth of the polymer melt and, accordingly, the height of the fabricated nanopillars. Particularly, by setting the "heating temperature" to 270, 300, 330, or 360 °C, nanopillars with heights of approximately 5.5, 16, 37, or 45 μm were fabricated, respectively (for fabrication of all samples, the "cooling temperature" was kept constant at the room temperature).^{5,6} At the low density of the top terminating layer (corresponding to the lowest temperature gradient), due to the high AR of nanopillars ($\text{AR} = 27.5$), the nanopillars collapsed at the tip and formed an island-like structure (see Figure 3A). However, by increasing the density of the hierarchical level on top (see Figures 3B and 3C), extremely high AR nanopillars ($\text{AR} = 80$ and 185 , respectively) were fabricated. For taller pillars ($\text{AR} = 225$), although the terminating

nanostructure was very dense, due to its small size, the top layer could not hold itself together and the characteristic self-sticking of pillars at the walls led to the bundling of pillars into an island-like structure, but this time at the cost of shrinkage of the top nanolayer.^{5,6} It is worthwhile mentioning that keeping the "heating temperature" constant while changing the "cooling temperature" allows the fabrication of bi-level Teflon AF nanopillars of identical heights but with terminating nanostructures of distinct geometrical properties. However, for the sake of brevity, the cases where the "cooling temperature" was changed will not be discussed in the current report.

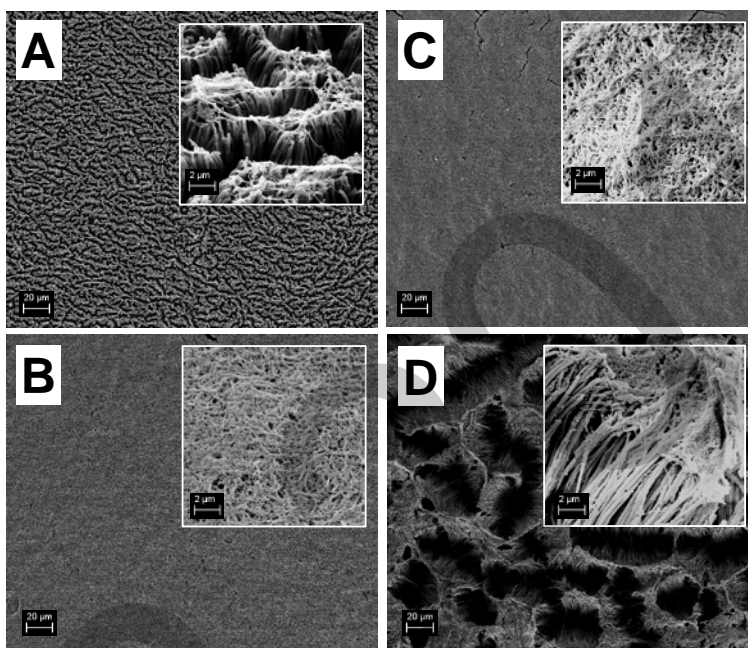


Figure 3. SEM images of bi-level Teflon AF nanopillars of different geometrical properties; nanopillars with different heights of approximately A) 5.5 μm , B) 16 μm , C) 37 μm , and D) 45 μm , have been fabricated by setting the "heating temperature" to 270, 300, 330, and 360 $^{\circ}\text{C}$, respectively ("cooling temperature" was kept constant at the room temperature). The images show the top-view of the samples while the magnified images are from the 45 $^{\circ}$ -view.⁶

The adhesive and frictional properties of the fabricated nanopillars as well as those of the flat Teflon AF (as the control sample) were characterized by indentation and load-drag-pull (LDP) tests, respectively. The tests were performed using an 8 mm in diameter hemispherical fused silica (ISP Optics Corp.) probe. The same as with flat control samples, negligible pull-off forces were detected for the tallest nanopillars (sample D; $\sim 45 \mu\text{m}$ tall), which were attributed to the collapse and bundling of the nanopillars and accordingly the very small actual area of contact (see Figure 4).^{5,6,8-10} However, for one level shorter nanopillars (sample C; $\sim 37 \mu\text{m}$ tall) which did not collapse at the tip because of the presence of the terminating layer on top, substantial pull-off forces were detected while still lower than those for sample B with nanopillars of $\sim 16 \mu\text{m}$ tall. Even though sample B had a lower surface area available for contact in comparison to sample C (as detected by water contact angle measurement tests), it showed a remarkably superior adhesion performance, most likely due to a lower chance of buckling during loading because of the lower height compared to the 37 μm tall pillars.^{5,6,8-10} Sample B reached the astonishing adhesion strength value (pull-off force per unit surface area) of $\sim 1.6 \text{ N/cm}^2$, while sample C showed a lower efficiency (i.e., adhesion strength of $\sim 1.1 \text{ N/cm}^2$), although both

performed better than a gecko foot pad (see Figure 4).^{5,6} As the height decreased further (sample A, $\sim 5.5 \mu\text{m}$ tall), it was observed that the pillars showed remarkable adhesive properties at low preloads, while at higher preloads their efficiency in generating adhesion compared to more flexible taller pillars was lower, as expected.^{5,6,8} The $5.5 \mu\text{m}$ tall nanopillars showed very high achievable adhesion strength of $\sim 1.3 \text{ N/cm}^2$ at a very small preload of $\sim 12 \text{ mN}$.

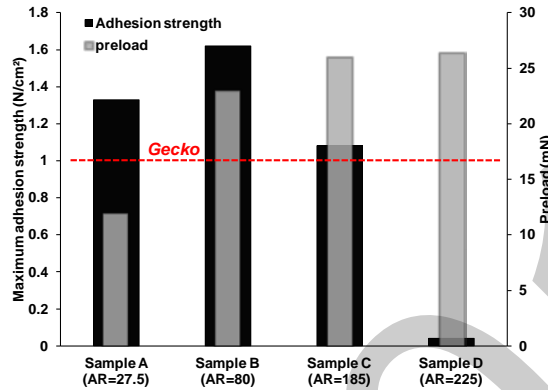


Figure 4. The adhesion strength and the corresponding preload for bi-level nanopillars with different heights of ~ 5.5 , 16, 37, and $45 \mu\text{m}$ (samples A, B, C, and D, respectively); the red dashed line shows the normal adhesion strength of natural gecko (1 N/cm^2).⁶

Due to the geometrical properties of the shortest nanopillars (i.e., low density of the hierarchical level), these nanopillars can make an effective sidewall contact with the fused silica probe (see Figure 3A), most likely leading to their observed improved effective shear strength as observed in LDP tests;^{5,6} sample A reached the remarkable shear strength value of $\sim 12 \text{ N/cm}^2$ at a 25 mN preload (Figure 5), $\sim 20\%$ higher than that of a natural gecko (i.e., 10 N/cm^2).

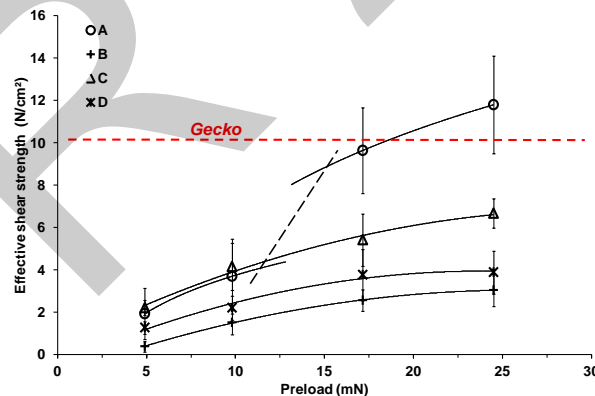


Figure 5. Effective shear strength at the start of the dragging step in LDP tests for bi-level Teflon AF nanopillars with different heights of ~ 5.5 , 16, 37, and $45 \mu\text{m}$ (samples A, B, C, and D, respectively) at nominal preloads of 5, 10, 17.5, and 25 mN. The red dashed line shows the shear strength of natural gecko (10 N/cm^2) reported in the literature.⁶

Even though for mid-sized nanopillars the elevated density of the top terminating layer hindered the sidewall contact, the sheet-like structure of the top layer helped these nanopillars to still generate large shear strength values (up to ~ 3 and 7 N/cm^2 for samples B and C, respectively).^{5,6} In comparison to these nanopillars, the bundled $45 \mu\text{m}$ tall nanopillars (sample D) reached a relatively moderate effective shear strength (up to $\sim 4 \text{ N/cm}^2$), most likely due to their ability to

generate minor sidewall contact with the probe (see Figure 5), even though they still had a low actual surface area because of the bundling effect.^{5,6,8,9}

In summary, we reported the fabrication of bi-level Teflon AF fibrillar nanostructures of various geometrical properties, as a new generation of dry adhesives. These nanostructures work based on electrostatic interactions at the surface rather than van der Waals forces (based on which most other dry adhesives are operating). By means of a novel fabrication method, the nanopillars were terminated at their top by a unique sheet-like nanostructure, effectively hindering the self-sticking of high-aspect-ratio and high-density nanopillars. The generated adhesion and friction strengths by these nanopillars not only matched those of gecko (a typically used upper limit from nature) but also surpassed them by ~60 and 20%, respectively.

References

1. H.T. Baytekin, A.Z. Patashinski, M. Branicki, B. Bay-tekin, S. Soh, B.A. Grzybowski, *Science*, **2011**, *333*, 308-312.
2. C. Liu and A.J. Bard, *Nature Materials*, **2008**, *7*, 505-509.
3. R.G. Horn and D.T. Smith, *Science*, **1992**, *256*, 362-364.
4. H. Izadi, B. Zhao, Y. Han, N. McManus, A. Penlidis, *Journal of Polymer Science Part B: Polymer Physics*, **2012**, *50*, 846-851.
5. H. Izadi, M. Golmakani, A. Penlidis, *Soft Matter*, **2013**, *9*, 1985-1996.
6. H. Izadi and A. Penlidis, *Proceedings of the 36th Annual Meeting of the Adhesion Society*, **2013**, March 3-6, Daytona Beach, FL, USA.
7. J. Scheirs, *Modern Fluoropolymers: High Performance Polymers for Diverse Applications*, **1997**, John Wiley & Sons, Chichester.
8. C. Greiner, A. del Campo, E. Arzt, *Langmuir*, **2007**, *23*, 3495-3502.
9. N.J. Glassmaker, A. Jagota, C.Y. Hui, J. Kim, *Journal of the Royal Society Interface*, **2004**, *1*, 23-33.
10. A.K. Geim, S.V. Dubonos, I.V. Grigorieva, K.S. No-voselov, A.A. Zhukov, S. YU. Shapoval, *Nature Materials*, **2003**, *2*, 461-463.

How to Make a Fluoropolymer Sticky!

Hadi Izadi and Alexander Penlidis

Institute for Polymer Research (IPR), Department of Chemical Engineering, University of Waterloo
Waterloo, ON, Canada

May 08, 2013

1

Outline

- Introduction
- Fabrication
- Adhesion and Friction
- Current and Future Work



2

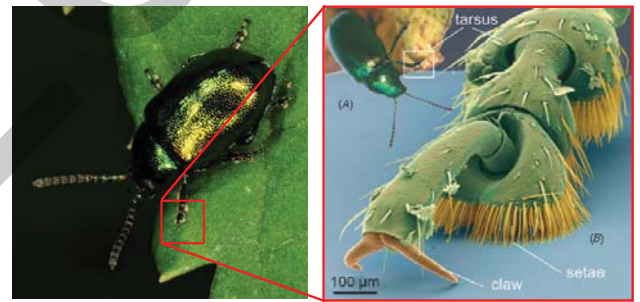
Introduction



3

Introduction

- Biological adhesives:



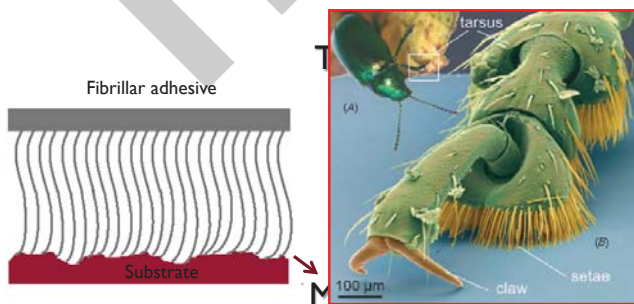
Green dock beetle

Gorb et al. *Bioinspir. Biomim.* 2007

4

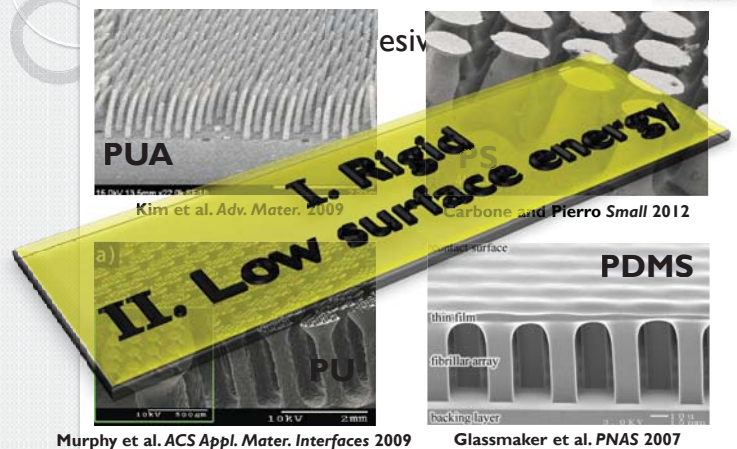
Introduction

- Biological adhesives:



5

Introduction



Murphy et al. *ACS Appl. Mater. Interfaces* 2009

Glassmaker et al. *PNAS* 2007

6

Introduction

Fluoropolymers (e.g., Teflon)

Very low surface energy Low electronegativity

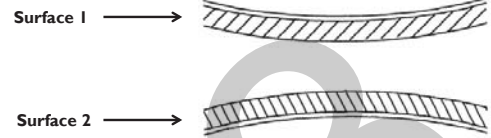
Weak van der Waals interactions



Strong electrostatic interactions

Introduction

Contact Electrification



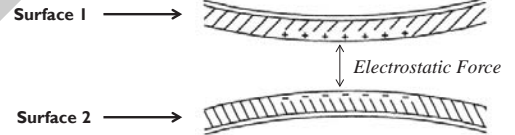
Introduction

Contact Electrification



Introduction

Contact Electrification



Introduction

Real contact area ↑

Compliant surface

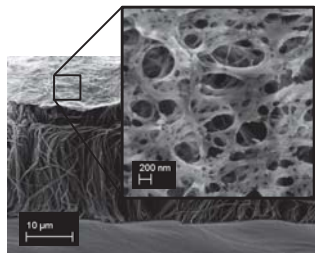
Surface charge density ↑

Insulating material

Terminating nanostructure

High aspect-ratio (AR) nanopillars

Backing layer

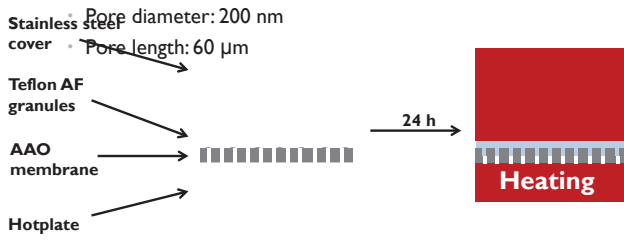


Fabrication



Fabrication

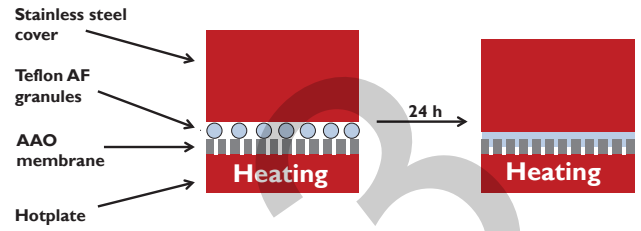
- Replica-molding
 - Polymer: Teflon AF
 - Mold: Anodic Aluminum Oxide (AAO) Membrane



13

Fabrication

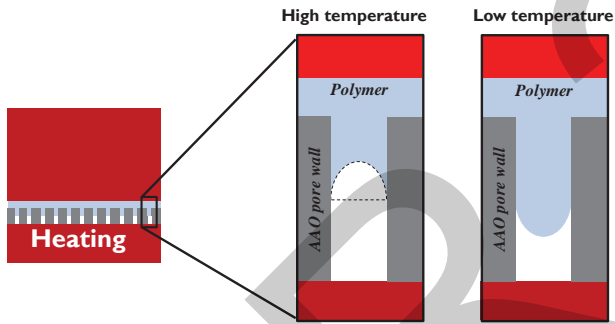
- Replica-molding



14

Fabrication

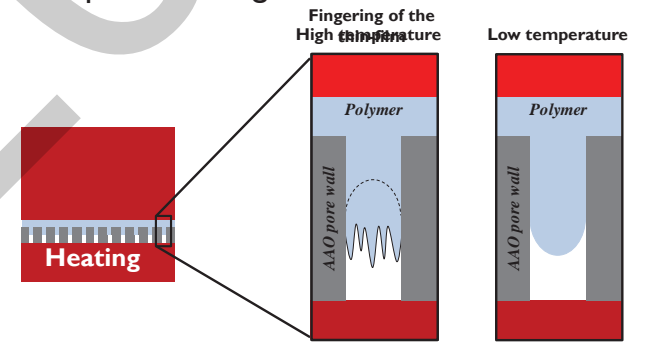
- Replica-molding



15

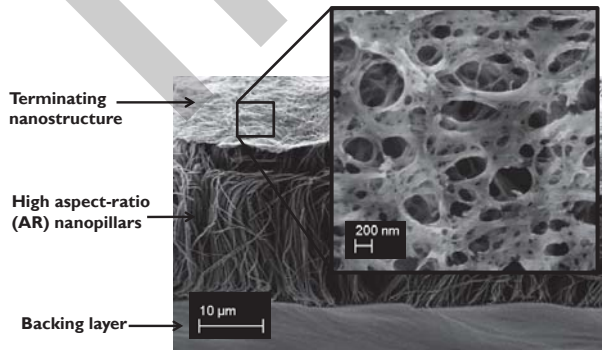
Fabrication

- Replica-molding



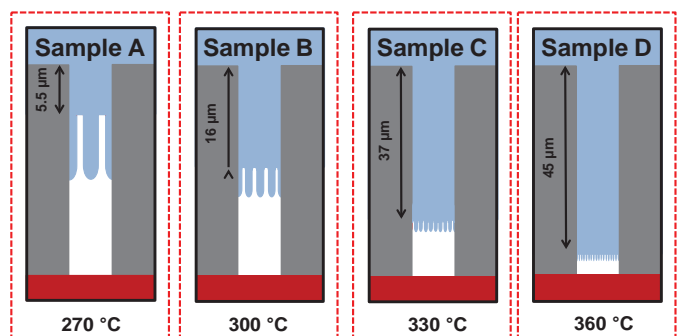
16

Fabrication



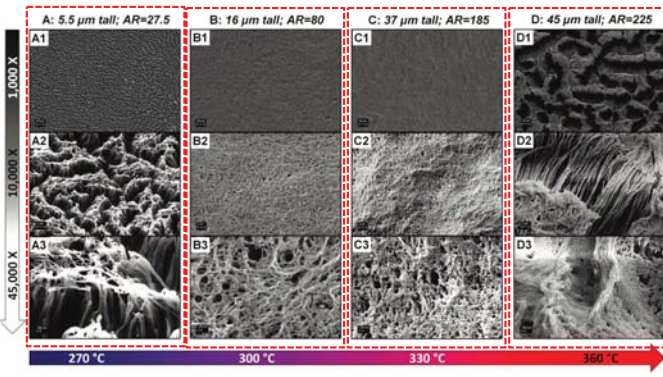
17

Fabrication



18

Fabrication



Izadi et al. *Soft Matter* 2013

Adhesion & Friction



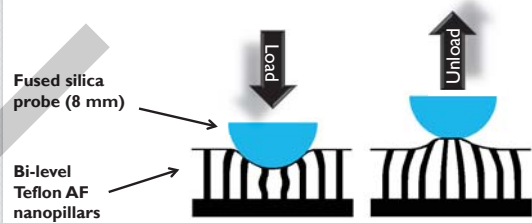
Adhesion & Friction



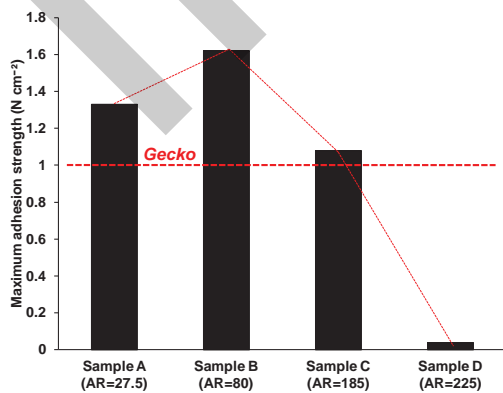
Adhesion & Friction



Adhesion: Indentation tests



Adhesion & Friction



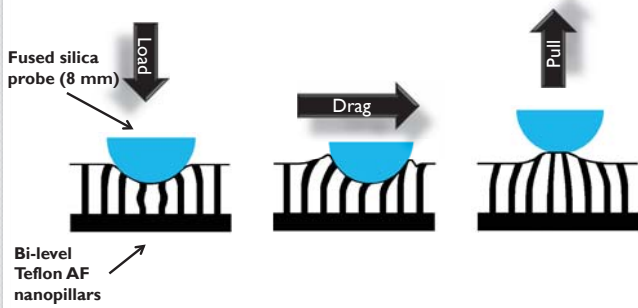
Izadi et al. *Soft Matter* 2013

Adhesion & Friction



Adhesion & Friction

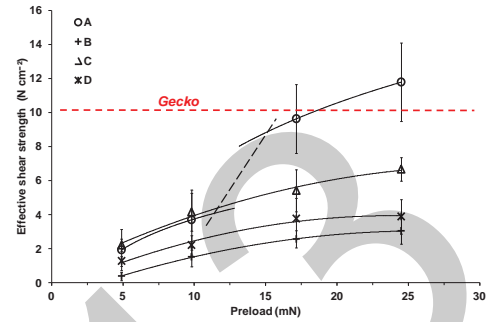
- Friction: Load-Drag-Pull (LDP) tests



25

Adhesion & Friction

- Start of dragging:



Izadi et al. Soft Matter 2013

26

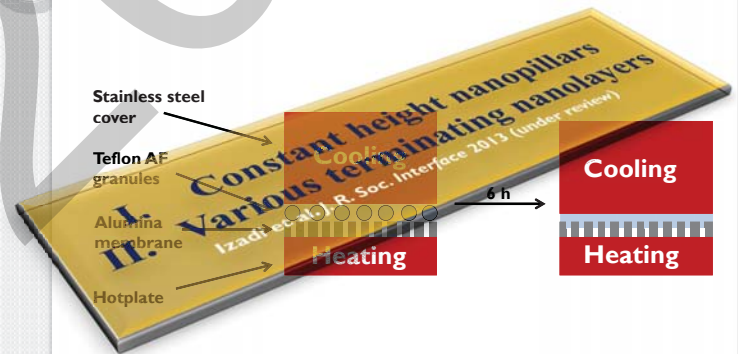
Current & Future Work



27

Current & Future Work

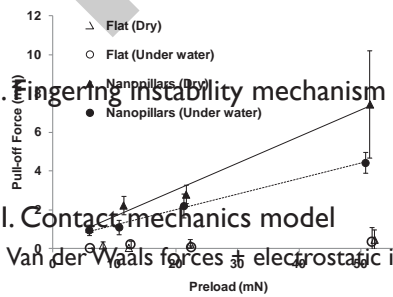
- Current work



28

Current & Future Work

- Future work
 - I. Underwater adhesion



- II. Fingerting instability mechanism
- III. Contact mechanics model
 - Van der Waals forces + electrostatic interactions

Izadi et al. J. Polym. Sci., Part B: Polym. Phys. 2012

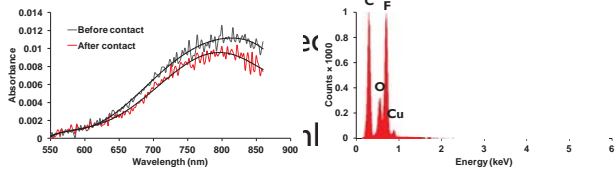
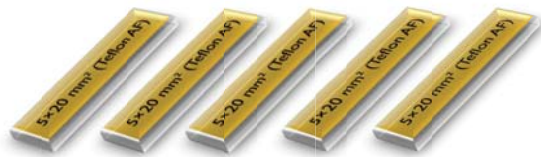
29

THANK YOU!



30

Contact Electrification



Izadi et al. Soft Matter 2013

Introduction

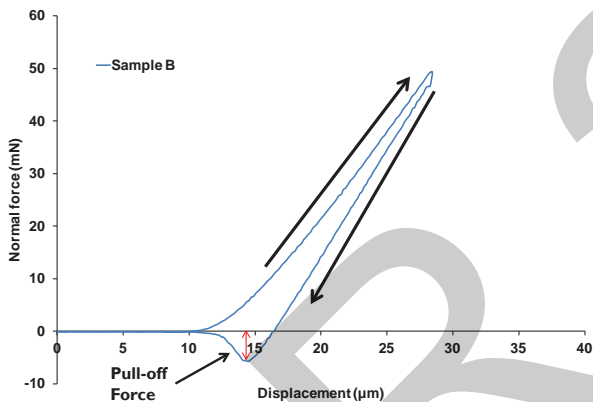
Contact Electrification

$$\text{Electrostatic Force} = -\frac{a_{con} \sigma^2}{2\epsilon_0 \epsilon_r}$$

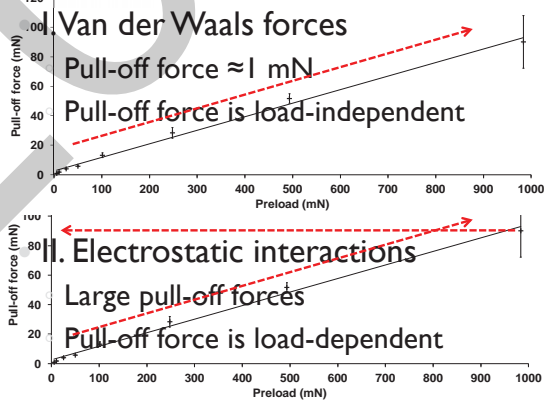
Surface charge density
 Permittivity of free space
 Permittivity of separating medium



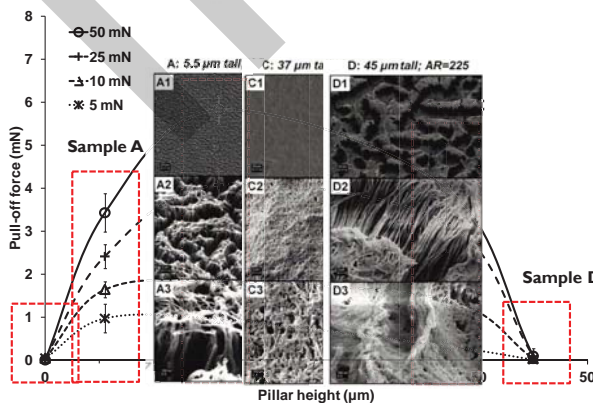
Adhesion & Friction



Adhesion & Friction



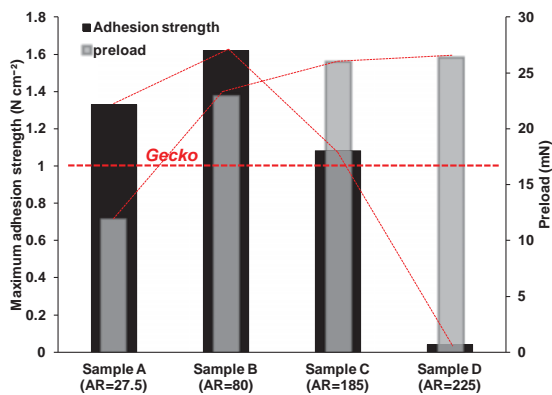
Adhesion & Friction



Flat Teflon AF

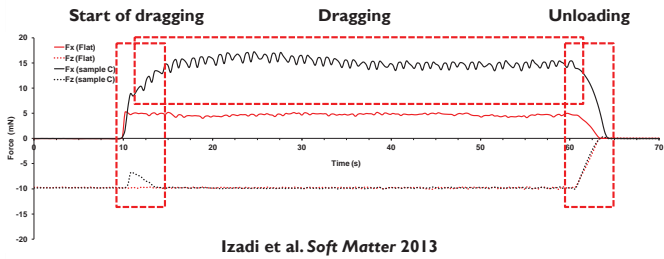
Izadi et al. Soft Matter 2013

Adhesion & Friction



Izadi et al. Soft Matter 2013

Adhesion & Friction

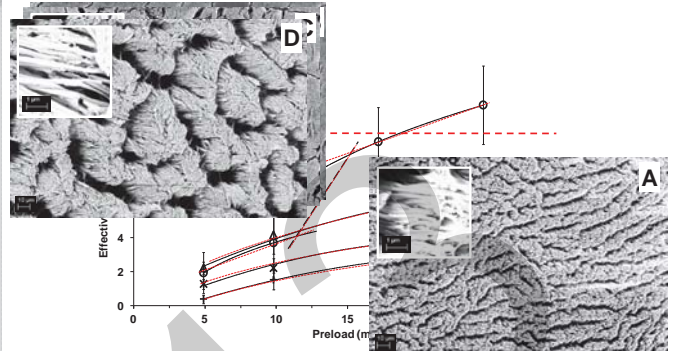


Izadi et al. *Soft Matter* 2013

Adhesion & Friction



- Start of dragging:

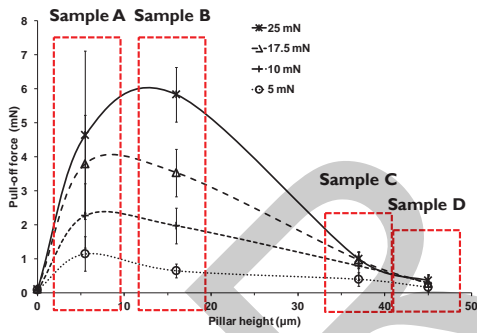


Izadi et al. *Soft Matter* 2013

Adhesion & Friction



- Unloading:



Izadi et al. *Soft Matter* 2013